JOURNAL OF Materials CHEMISTRY

Preparation of the negative thermal expansion material cubic $ZrMo_2O_8$

Cora Lind,[a] Angus P. Wilkinson,*[a] Claudia J. Rawn[b] and E. Andrew Payzant[b]

[a]*School of Chemistry & Biochemistry, Georgia Institute of Technology, Atlanta, GA 30332-0400, USA. E-mail: angus.wilkinson@chemistry.gatech.edu*
[b]*Metals and Ceramics Division, Oak Ridge National Laboratory, Oak Ridge, TN 37831-6064, USA*

Received 15th May 2001, Accepted 27th July 2001
First published as an Advance Article on the web 27th September 2001

The negative thermal expansion material cubic $ZrMo_2O_8$ can be prepared by the carefully controlled dehydration of $ZrMo_2O_7(OH)_2{\cdot}2H_2O$. The quality of the end product is dependent upon the route used to prepare the $ZrMo_2O_7(OH)_2{\cdot}2H_2O$. The influence of both the Zr : Mo ratio in the solution used to prepare the hydrate and the type of acid used in its preparation (HCl, H_2SO_4, CH_3CO_2H, HNO_3 and $HClO_4$) are examined. Not all acids provide media suitable for the preparation of $ZrMo_2O_7(OH)_2{\cdot}2H_2O$. Cubic $ZrMo_2O_8$ could only be obtained from precipitates containing the hydrate. Starting solutions with a Zr : Mo ratio in excess of 1 : 2 were necessary to avoid coprecipitation of amorphous MoO_3. The nature of the acid used in the hydrate synthesis affects the morphology of both the hydrate precursor and the cubic $ZrMo_2O_8$ particles. Many of the syntheses examined led to cubic $ZrMo_2O_8$ contaminated with amorphous impurities. Highly crystalline pure material could be obtained by using a perchloric acid medium for the synthesis of the hydrate precursor.

1. Introduction

Negative thermal expansion (NTE) materials have received considerable attention during the last decade.[1–3] Their use in composites may facilitate control of thermal expansion and should in principle allow the design of materials with a specific expansion coefficient anywhere between the values of the pure components of the composite. Matching the thermal expansion of device parts can be important to avoid cracks or separation at interfaces between two components, and zero expansion is needed when exact positioning of electronic or optical components in a device is crucial. It has recently been demonstrated that the use of a composite containing the NTE material cubic ZrW_2O_8 can prevent the expansion of optical fiber gratings.[4]

Prior to the recent interest in NTE materials, several families of compounds had been investigated because of their low expansion coefficients. Prominent examples are Invar,[5] lithium aluminium silicates (LAS)[6] and the $NaZr_2P_3O_{12}$ (NZP) family.[7,8] Materials based on LAS and NZP ceramics or glasses have found a wide variety of uses.[9,10] However, some applications require NTE (*e.g.* temperature compensation of optical fibers),[4] and others demand zero thermal expansion along with another property (*e.g.* insulator, conductor, strength, flexibility *etc.*) that may not be intrinsic to the low expansion material. This makes the use of NTE materials as fillers in composites attractive, as they can counterbalance the normal positive expansion of the matrix material while the matrix provides some valuable property. The recent work on Cu/ZrW_2O_8 composites is an example of this approach.[11,12]

An ideal NTE material should undergo isotropic and preferably linear negative expansion over a large temperature range including room temperature.[2] It should also be accessible from cheap, commercially available precursors and easy to prepare. For use in composites, it is desirable that the material is thermodynamically stable over a large temperature and pressure range. The material should not undergo phase transitions at low pressures, as the composite matrix may compress the filler during processing and use.

In reality, no known material fulfills all of these requirements. The most promising NTE materials to date can be grouped into three families: the $Sc_2W_3O_{12}$ family,[13–16] the ZrV_2O_7 family,[17–19] and the ZrW_2O_8 family.[20–23] The first class of compounds crystallizes with orthorhombic or monoclinic symmetry, so that the expansion behavior is never truly isotropic, although it can be close to isotropic in some cases. Both of the other families show cubic symmetry, but most compounds related to ZrV_2O_7 exist with a $3\times3\times3$ superstructure at room temperature, which exhibits positive thermal expansion. Negative thermal expansion thus only occurs above room temperature. The NTE of ZrW_2O_8 was first observed by Martinek and Hummel in the temperature range 50–700 °C in 1968.[24] Little attention was paid to this material until Sleight's group solved its crystal structure in 1996 and extended the temperature range of the expansion measurements, showing that cubic ZrW_2O_8 contracts on heating between 0.3 and 1050 K.[21] Unfortunately, there are some drawbacks to this material. ZrW_2O_8 is only thermodynamically stable at high temperatures.[21] The expansion curve shows a discontinuity around 430 K, where the material undergoes a cubic-to-cubic phase transition (α to β). This changes the linear expansion coefficient from -8.8 to -4.9×10^{-6} K^{-1}.[20] Perhaps the most severe limitation, however, is a phase transition to an orthorhombic structure (γ-ZrW_2O_8) at 0.21 GPa that is not reversible at ambient temperature.[25,26] It was the formation of this phase that led to problems during the processing of ZrW_2O_8/Cu composites.[11,12]

We have previously reported the first synthesis of cubic $ZrMo_2O_8$ by the dehydration of $ZrMo_2O_7(OH)_2{\cdot}2H_2O$.[23] However, this synthesis was far from optimal. Cubic $ZrMo_2O_8$ is isostructural with β-ZrW_2O_8 and displays NTE with $\alpha=-5.0\times10^{-6}$ K^{-1} between -262 and $+300$ °C. No phase transitions are observed in this temperature range. There is a reversible phase transition at pressures between 0.7 and 2.0 GPa.[27] The complete reversibility and higher onset pressure of this transition might be advantageous for applications in composites.

 DOI: 10.1039/b104283c

Unfortunately, cubic $ZrMo_2O_8$ appears to be metastable at all temperatures with regard to other polymorphs of $ZrMo_2O_8$. This leads to considerable difficulties in the synthesis of phase pure cubic material. The only known synthetic pathway is the dehydration of $ZrMo_2O_7(OH)_2{\cdot}2H_2O$,[28] which has been obtained by the reaction of water soluble molybdenum and zirconium compounds. Minor changes in the preparation method can have a considerable effect on the exact crystallization behavior as well as the sample morphology.

In this paper, we examine the influence of the zirconium to molybdenum ratio in the starting solution and the effect of different zirconium starting materials on the ease of preparation and properties of cubic $ZrMo_2O_8$. The ratio of zirconium to molybdenum in the starting solution was varied between 1 : 2 and 2.5 : 2. Syntheses were carried out in sulfuric, acetic, hydrochloric, nitric and perchloric acids. Appropriate conditions for the synthesis of stoichiometric precursor precipitates as well as conditions that facilitate the crystallization of pure cubic $ZrMo_2O_8$ are reported.

2. Experimental

2.1 Materials

Precursor precipitates were synthesized from $(NH_4)_6Mo_7O_{24}{\cdot}4H_2O$ (J. T. Baker or Aldrich) and zirconyl perchlorate hydrate, zirconyl nitrate hydrate, zirconium acetate hydroxide, zirconium sulfate hydrate (Aldrich) or zirconyl chloride hydrate (Strem, Alpha Aesar). The metal contents of all the starting materials were determined gravimetrically. Half concentrated acids were prepared by 1 : 1 dilution with distilled water from the corresponding concentrated acids purchased from J. T. Baker (HCl, HNO_3 and H_2SO_4) and Fisher ($HClO_4$, HNO_3 and CH_3CO_2H). The resulting HCl, HNO_3, H_2SO_4, $HClO_4$ and CH_3CO_2H solutions had concentrations of approximately 6 M, 8 M, 9 M, 6 M and 9 M respectively.

2.2 Synthesis of the Zr/Mo precipitates

For each Zr starting material, precipitates were prepared from solutions with a nominal 1 : 2 Zr : Mo stoichiometry and from solutions containing excess Zr. In all cases, the anion present in the Zr starting material was matched with that of the acidic synthesis medium (*e.g.* $ZrOCl_2$ and HCl). All preparations were carried out as described in the next paragraph.

In two separate Erlenmeyer flasks, 15 mmol (between 18 and 37.5 mmol for the excess Zr samples) Zr starting material and 4.286 ($\equiv$30/7) mmol $(NH_4)_6Mo_7O_{24}{\cdot}4H_2O$ were each dissolved in 30 mL water. The two solutions were simultaneously dripped into 20 mL water while stirring. With the exception of the experiments using acetate, a white precipitate formed. After stirring at room temperature for several hours, 80 mL of the appropriate half concentrated acid were added while continuing the stirring. The precipitates dissolved in all cases. The mixtures were then refluxed for three days. The sulfate solutions remained clear, while precipitates formed in all of the other experiments. The precipitates were white for the chloride and acetate systems, pale yellow for the nitrate route and pale blue or white for the perchlorate systems. The mixtures were cooled to room temperature and the precipitates separated by centrifugation. They were resuspended in distilled water and centrifuged several times until the pH of the liquid was $\sim$4–5. For the sulfate samples, NH_3 was added to the cooled solutions in order to obtain a precipitate at pH $\sim$ 5. The powders were dried between room temperature and 70 °C and subsequently characterized.

As there was some batch-to-batch variation in samples prepared using nominally the same precursor chemistry, several samples synthesized by the successful perchlorate, nitrate and chloride routes were examined to give a representative picture.

Table 1 Overview of Zr excess levels and yields for all the precursors employed. Yields were calculated based on the amount of molybdenum in the starting solution and assuming a $ZrMo_2O_7(OH)_2{\cdot}2H_2O$ precipitate

	No. of samples and % yield				
Excess of Zr (%)	$CH_3CO_2^-$	SO_4^-	Cl^-	NO_3^-	ClO_4^-
0	2 89–97	2 65–70	4 72–106	4 91–93	1 99
20	N/A	N/A	1 98	N/A	N/A
32	N/A	N/A	N/A	N/A	1 97
40	N/A	N/A	1 94	N/A	N/A
60	N/A	N/A	1 98	N/A	N/A
63	2 105–115	2 94	7 91–100	6 60–82	3 92–95
70	N/A	N/A	N/A	N/A	4 87–93
100	N/A	N/A	N/A	1 61	N/A
150	N/A	N/A	N/A	1 68	N/A

In this paper, results from 17 chloride precursor, 12 nitrate precursor, and 9 perchlorate precursor samples are discussed. Table 1 gives an overview of the Zr excess levels and the yields of precipitates that were obtained.

2.3 Characterization

TGA/DTA measurements on the as-recovered materials were conducted using a Seiko 320 instrument with nitrogen as the carrier gas. All experiments were carried out between 30 and 1200 °C with a heating rate of 20 °C min^{-1} and a 15 min hold time at 1200 °C.

The samples were characterized by X-ray diffraction prior to heat treatment and after various heat treatments to investigate their crystallization behavior. For the room temperature measurements, a Scintag X1 diffractometer with a Peltier cooled solid-state detector and a copper tube was used. Amorphous content analyses were performed for some samples by mixing the cubic material with a silicon standard (Alfa Aesar, 99.5% purity silicon powder, crystalline, −325 mesh). A high quality XRD pattern was collected on this mixture as well as on the same mixture after heating to 600–700 °C overnight to ensure complete crystallization of the trigonal polymorph. Phase fractions were extracted from both patterns by Rietveld analysis using GSAS,[29] and the relative values for the cubic and trigonal phases were compared to estimate the amount of amorphous material in the cubic sample. This approach assumes that all of the amorphous material in the cubic sample is converted to crystalline trigonal $ZrMo_2O_8$ on heating to 600–700 °C overnight, and it was adopted because the error associated with the absorption mismatch between the silicon internal standard and the zirconium molybdate is largely eliminated.

XRD data were also collected as a function of sample temperature. Data were acquired for 30 s at 20 °C intervals. During data acquisition the temperature was held constant. The sample was then heated at 40 °C min^{-1} to get to the next temperature for data collection. This heating-rate–hold-time combination was chosen so that the average heating rate of the XRD experiments matched that used in the TGA/DTA experiments (20 °C min^{-1}). The measurements were performed using a Scintag PAD X diffractometer with a copper tube and an mBraun linear position sensitive detector (PSD)[30] covering a 10° range centered at 26° 2θ. A Bühler HDK2.3 accessory equipped with a Pt–20%Rh heater strip and a type S thermocouple was used to heat the samples.[31]

The sample morphology and particle size were examined with a Hitachi S800 FEG scanning electron microscope. SEM images were taken for all the as-prepared precipitates (the powders recovered from the reaction mixtures as described in section 2.2).

3. Results

Powder diffraction indicated that the raw precipitates recovered from the preparations using hydrochloric, nitric or perchloric acid contained crystalline $ZrMo_2O_7(OH)_2 \cdot 2H_2O$. Heat treatment of these precipitates led to the crystallization of the previously reported LT polymorph,[23] cubic, or trigonal $ZrMo_2O_8$, or a mixture of these phases. Precipitates prepared *via* the sulfate route were amorphous and crystallized at around 600–650 °C to either trigonal $ZrMo_2O_8$ or a mixture of the trigonal phase and monoclinic ZrO_2 (in samples prepared with excess Zr). The acetic acid route resulted in powders with an as yet unidentified structure, which transformed to trigonal $ZrMo_2O_8$ when heated to 500–600 °C. Heating the precipitates obtained from both the sulfate and acetic acid routes never produced any cubic $ZrMo_2O_8$. This result suggests that the formation of the LT polymorph is a crucial step for the crystallization of cubic $ZrMo_2O_8$. The unsuccessful sulfate and acetate precursor routes will not be discussed any further.

3.1 Thermal analysis experiments

All the TGA curves showed a large weight loss due to dehydration between 100 and 200 °C and a high temperature weight loss between 850 and 1030 °C (see Fig. 1). For some samples, another weight loss was observed between 700 and 750 °C (see Fig. 1a). These weight losses can be assigned to the evaporation of framework MoO_3 from $ZrMo_2O_8$ and a MoO_3 impurity phase. MoO_3 evaporates at around 750 °C, while ternary or quaternary compounds are often stable to slightly higher temperatures.

Sample compositions were calculated using the final weights and the weights of the dehydrated materials obtained by TGA. The precipitates prepared from solutions with a 1 : 2 Zr : Mo ratio were found to be Mo rich for all three Zr starting materials (Zr : Mo between 0.88 : 2.00 and 0.97 : 2.00). Excess Mo was also observed in the samples prepared in nitric acid with less than 100% excess Zr and in samples prepared in perchloric acid with up to 63% excess Zr. All the other precipitates were stoichiometric within experimental error. However, some samples from the chloride route showed a weight loss at 750 °C despite the calculated 1 : 2 stoichiometry. This suggests that they contained a 1 : 2 mixture of "ZrO_2" and "MoO_3" impurities.

The DTA curves showed the expected endothermic peaks corresponding to the weight losses, and two exothermic peaks for each sample, which can be assigned to the crystallization of cubic and trigonal $ZrMo_2O_8$, respectively (see Fig. 1). The temperatures of the endothermic events as well as the crystallization of the trigonal phase (500–540 °C for chloride and nitrate, 520–560 °C for perchlorate) were independent of solution stoichiometry. Due to the higher formation temperature of the trigonal phase, the separation of the two exothermic peaks was very large for all of the samples produced in perchloric acid (between 65 and 110 °C). For the cubic phase, the lowest crystallization temperatures were observed for samples prepared from solutions with 1 : 2 Zr : Mo ratios (410–465 °C). The crystallization temperatures increased with increasing zirconium content and remained in the 460 to 490 °C range for all samples that were stoichiometric. For a few samples, higher temperatures of 500 and 520 °C were observed. These samples also showed higher peak temperatures for the cubic to trigonal transformation (550 and 565 °C, respectively).

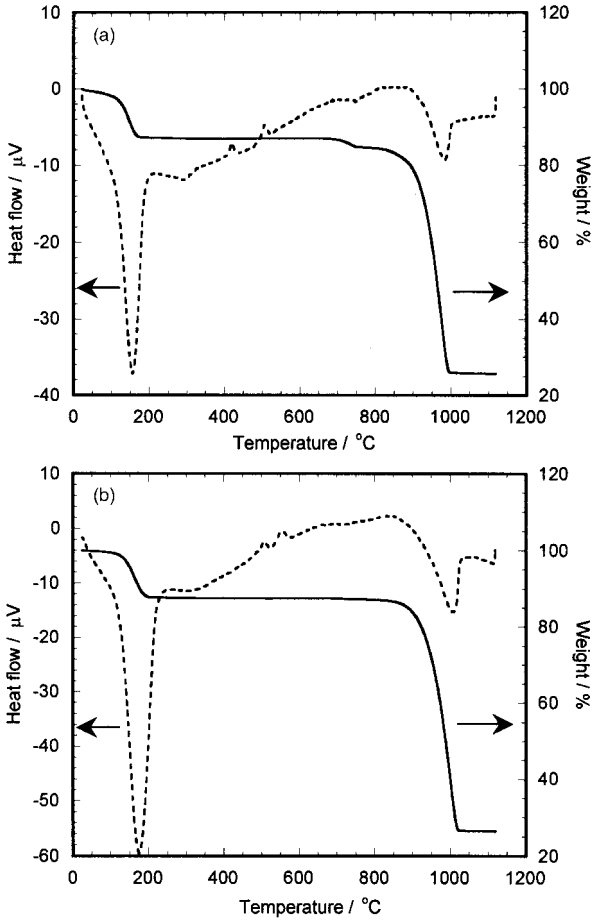

Fig. 1 Typical TGA/DTA curves for (a) hydrate samples that will give cubic material without trigonal impurities and (b) samples that will always yield a mixture of cubic and trigonal phase. The weight loss around 750 °C in (a) is due to the presence of excess MoO_3.

3.2 Crystallization studies

Ex situ X-ray diffraction experiments showed that all of the raw precipitates from the chloride, nitrate, and perchlorate routes contained crystalline $ZrMo_2O_7(OH)_2 \cdot 2H_2O$. Upon dehydration, the previously reported low temperature polymorph ("LT" $ZrMo_2O_8$) was formed.[23] Further heating to temperatures between 355 and 410 °C resulted in the crystallization of cubic $ZrMo_2O_8$. For some samples, heat treatment for an extended time period in the temperature range 355–365 °C led to complete conversion of the LT polymorph, while others required heating to higher temperatures for short time periods. The factors that influence the crystallization are complex. Of the samples prepared with excess Zr in hydrochloric acid, five gave cubic $ZrMo_2O_8$ with no trigonal impurities, whereas the others contained varying amounts of the trigonal phase, less than 5% (6 samples), 10–20% (2 samples), and 50% (1 sample). In the samples prepared using a 1 : 2 Zr : Mo ratio in solution, residual MoO_3 was observed as a second crystalline phase at high temperatures. However, a 1 : 2 Zr : Mo ratio in the starting solution typically facilitated the preparation of cubic material without trigonal impurities. Three of the four samples showed no trigonal impurities, the last sample gave 5% trigonal phase. Most samples contained ~5–10% of an amorphous "$ZrMo_2O_8$" phase along with the cubic material.

For the nitrate route, cubic materials without trigonal impurities could be crystallized if the metal ratio in solution was 1 : 2. None of the samples prepared with excess zirconium could be converted to the cubic phase without at least 10% trigonal content. The amount of trigonal material increased with increasing excess of zirconium in the preparation. A

typical sample from the nitrate route contained ~15–20% amorphous "$ZrMo_2O_8$".

All samples prepared *via* the perchlorate route could be converted to highly crystalline cubic material without trigonal impurities when heated to between 365 and 405 °C. The two samples prepared from starting mixtures with a 1 : 2 Zr : Mo ratio and with 32% excess Zr also contained crystalline MoO_3. Cubic $ZrMo_2O_8$ free from amorphous and crystalline impurities was obtained from precursors prepared using 63–70% excess Zr.

The evolution of the XRD patterns on heating two representative samples precipitated from hydrochloric acid with a 1 : 2 metal ratio in solution and with 63% excess zirconium respectively is shown in Fig. 2. Crystallization of the cubic phase started at a lower temperature for the sample prepared with a 1 : 2 metal ratio in solution (420 *vs.* 480 °C). The trigonal peaks were first observed at about the same temperature, 520 °C, for both samples. Thus, the 1 : 2 metal ratio leads to a 40 °C window in which the 1 : 2 sample showed cubic $ZrMo_2O_8$ as the only crystalline compound. In the excess Zr sample, there was always either LT or trigonal $ZrMo_2O_8$ present along with the cubic phase. This is in agreement with our inability to obtain phase pure cubic material from the latter sample. The crystallization temperatures for all phases agreed with the peak temperatures observed in the DTA curves within ±10 °C.

3.3 Particle size and morphology

All of the Zr/Mo precipitates consisted of submicron primary particles with different tendencies to agglomerate. Typical samples prepared in hydrochloric acid (see Fig. 3a) contained

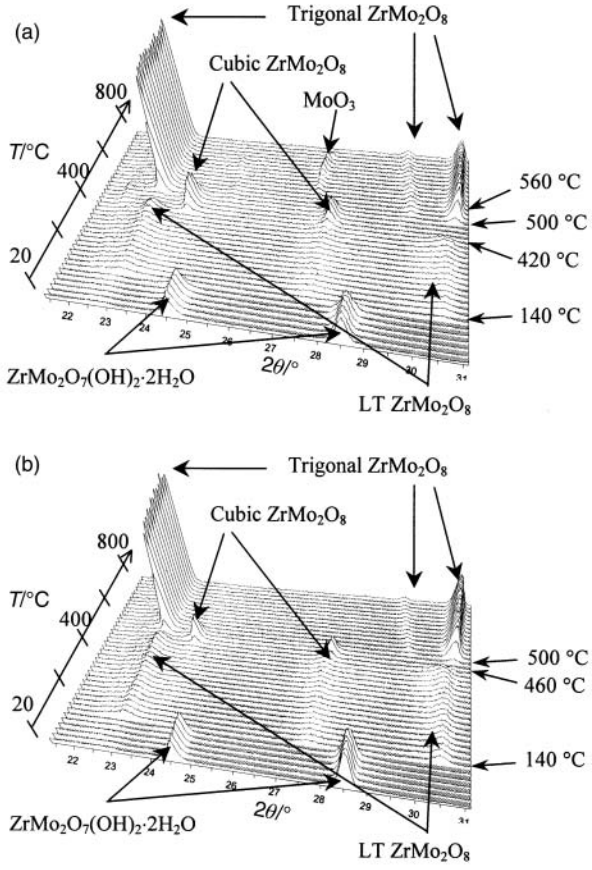

Fig. 2 XRD patterns obtained *in-situ* while heating hydrate samples prepared using the chloride route: (a) a sample prepared with a 1 : 2 metal ratio in solution and (b) a sample prepared with 63% excess zirconium. Patterns were collected between 20 and 800 °C at 20 °C intervals, using heating rates of 40 °C min^{-1} and 0.5 min acquisition time.

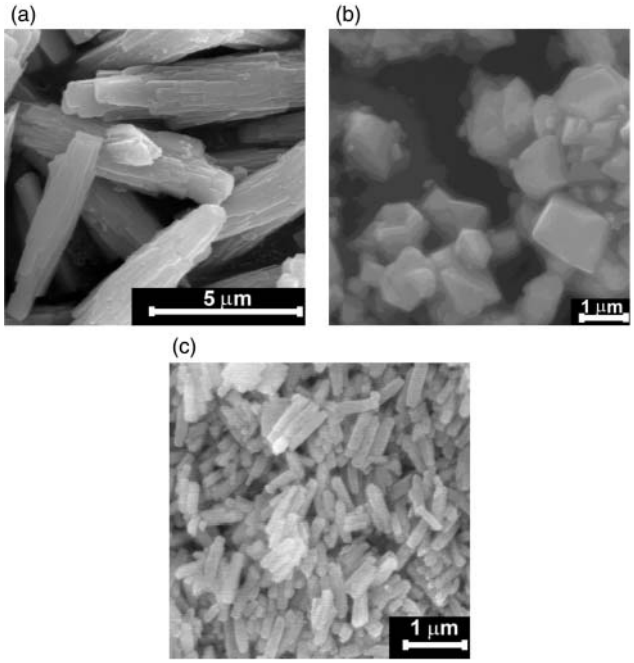

Fig. 3 SEM pictures of a) a sample prepared using chloride that shows agglomeration, b) a sample prepared using nitrate and c) a sample prepared using perchlorate.

rod like particles with diameters of 100–500 nm and lengths of up to several micrometers. The morphology was largely independent of the metal ratio in the starting mixture. In some samples, the rods formed rice grain like agglomerates with size distributions that varied from batch to batch. Samples prepared from a nitrate precursor consisted of equiaxed polyhedral particles in the size range 0.1–1 μm (see Fig. 3b). The polyhedra tended to agglomerate. The samples recovered from perchloric acid consisted of rod shaped particles with diameters of 200–500 nm and a length of up to several micrometers (see Fig. 3c). While these particles resemble the submicron rods observed in the samples obtained from the chloride route, little agglomeration was seen for this route.

4. Discussion

The results of this investigation corroborate the hypothesis that cubic $ZrMo_2O_8$ can only be obtained from $ZrMo_2O_7(OH)_2{\cdot}2H_2O$ *via* the LT polymorph. The use of $Zr(SO_4)_2$ or $Zr(OH)_x(CH_3CO_2)_y$ does not yield any $ZrMo_2O_7(OH)_2{\cdot}2H_2O$, and no cubic $ZrMo_2O_8$ could be synthesized using these starting materials. For all of the other precursors, the raw precipitate that was recovered primarily contained $ZrMo_2O_7(OH)_2{\cdot}2H_2O$, and heat treatment allowed the formation of the cubic phase *via* LT $ZrMo_2O_8$.

DTA proved to be a valuable method for the evaluation of the hydrate materials (see Fig. 1). Overlap of the two exotherms corresponding to the LT to cubic and cubic to trigonal transformations indicated that the synthesis of pure cubic $ZrMo_2O_8$ would be difficult or impossible, while a large separation between these peaks suggested relative insensitivity towards the exact heat treatment and time. Sharper DTA peaks indicated a well-defined narrow conversion range.

TGA offered a simple method for elemental analysis by evaporation of molybdenum oxide. The main advantage of this approach is that dissolution of the poorly soluble zirconium molybdates is not required. Excess zirconium in solution was necessary to obtain precipitates with a 1 : 2 Zr : Mo stoichiometry for the chloride, nitrate and perchlorate routes. All materials prepared using these routes showed a Zr : Mo ratio less than or equal to 0.5 despite the large excess of Zr that was

sometimes used in the starting mixture. This clearly demonstrated the higher solubility of zirconium in acid as compared to molybdenum. It is not known how high the excess of zirconium can be before additional zirconium is incorporated in the precipitate. In the case of samples prepared using perchlorate, a 63% excess of Zr in solution seemed to be near the lower limit for the preparation of stoichiometric precipitates. This was evident from the subtle changes between several samples prepared in this way. A Zr excess of 20% or more avoided the formation of Mo rich precipitates for the chloride precursor route. For the samples prepared using hydrochloric acid, an endothermic peak, due to the loss of non-framework MoO_3, was observed for several samples that were stoichiometric according to the total weight losses. This suggested that some precipitates contained phase separated amorphous "ZrO_2" and "MoO_3". Rietveld analyses on some cubic samples prepared by the chloride route revealed an amorphous content of ~5–10%, while no amorphous component was found in the cubic samples prepared using perchlorate. The nitrate route required a very large excess of zirconium for the formation of stoichiometric precipitates. It is interesting to note that the use of excess zirconium in the starting mixture increased the yield to >90% (calculation based on the amount of molybdenum in the starting mixture and a precipitate composition of $ZrMo_2O_7(OH)_2 \cdot 2H_2O$) on the chloride route, while the samples recovered from nitric acid gave such a yield with stoichiometric starting mixtures and gave lower values when excess zirconium was present. Perchlorate mixtures always led to more than 85% precipitation and showed no obvious trends with the metal ratio of the starting mixture.

All the precipitates produced in perchlorate media allowed the preparation of pure cubic $ZrMo_2O_8$ or a mixture of cubic $ZrMo_2O_8$ and MoO_3 regardless of the excess zirconium used, suggesting that this is the best route to cubic $ZrMo_2O_8$ that we have examined. Precipitates made using excess zirconium chloride produced either cubic or cubic/trigonal $ZrMo_2O_8$. None of the samples prepared with excess zirconium in a nitrate medium led to less than 10% trigonal $ZrMo_2O_8$. All cubic samples prepared from hydrochloric and nitric acid contained some amorphous material.

The crystallinity of the hydrates, as judged by the peak widths in the diffraction patterns, as well as that of the cubic materials increased in the order chloride < nitrate < perchlorate. High crystallinity hydrates favored the formation of phase pure cubic material. While the temperature needed for formation of the trigonal phase was largely independent of the zirconium excess level used during the preparation, a 1 : 2 Zr : Mo ratio in the starting mixtures led to lower crystallization temperatures for the cubic phase as compared to mixtures with excess zirconium in all three cases. This effect was less pronounced in the nitrate samples (20–30 °C lower DTA peak temperatures) than in the chloride and perchlorate samples (30–60 °C). The largest peak separation (80–110 °C) coupled with the lowest crystallization temperatures for the cubic phase (DTA peaks at 410–420 °C, 355–365 °C *ex situ*) was observed for samples prepared from mixtures with a 1 : 2 ratio of zirconyl perchlorate or zirconyl chloride and ammonium molybdate. All samples prepared from these 1 : 2 ratio solutions gave cubic material with no trigonal impurities. However, TGA revealed the presence of excess MoO_3.

As MoO_3 is easily soluble in dilute base, removal of the excess MoO_3 that was observed in some samples after heat treatment was attempted by washing the cubic materials with 0.05 M NaOH. The framework MoO_3 of $ZrMo_2O_8$ dissolves in stronger bases (*e.g.* 1 M NaOH), but no loss of framework molybdenum or crystal structure changes could be detected by TGA and XRD after treatment with 0.05 M NaOH. Unfortunately, this increased the amorphous component in the sample (from 15–20 to ~30% according to Rietveld analysis), making direct preparation from a stoichiometric hydrate favorable. An alternative approach would be an alkali wash of the hydrate followed by conversion of the stoichiometric material, but in our hands, base washed hydrates did not allow the preparation of more than minor amounts of cubic $ZrMo_2O_8$. The DTA curve showed only one broad peak at much lower temperatures than the peaks of the untreated material (see Fig. 4). This could either indicate that the excess MoO_3 plays an active role in the formation of cubic $ZrMo_2O_8$ or that changes in the microstructure inhibit the formation of cubic $ZrMo_2O_8$. The particle shape and size distribution remained unchanged during base washing, but the surface structure was affected. Whereas the raw hydrate and the as prepared cubic material showed well-defined polyhedra with smooth edges and surfaces, irregularities and cracks could be seen in the base washed hydrates and cubic materials.

The particle shape of the initial precipitates depended on the anions present in solution. Equiaxed polyhedra (NO_3^-), rods (ClO_4^-), and "rice grains" or rods (Cl^-) could be obtained. All samples showed primary particles with submicron size and different tendencies to agglomerate. The least aggregation was observed for the perchlorate samples. Dehydration and subsequent phase transformations to LT and cubic $ZrMo_2O_8$ did not change the particle morphology, while long-range diffusion seemed to occur during the cubic to trigonal conversion as evidenced by the changes in particle shape (see Fig. 5). For use in composites, particle shape could be an important consideration in both processing and use. The sample morphology will influence the mixing between matrix and filler and it may also have some influence on the occurrence of pressure gradients and possible pressure induced amorphization. The best particle shape was achieved on the nitrate route, while the agglomerated rods in the chloride samples could cause problems.

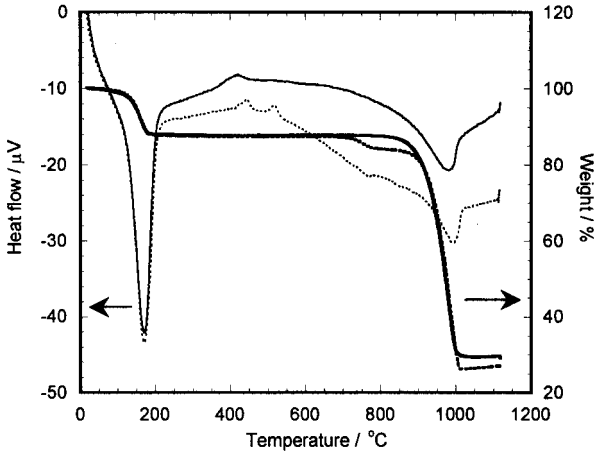

Fig. 4 TGA/DTA curves for a hydrate sample prepared using nitrate before (dotted lines) and after (solid lines) washing with 0.05 M NaOH.

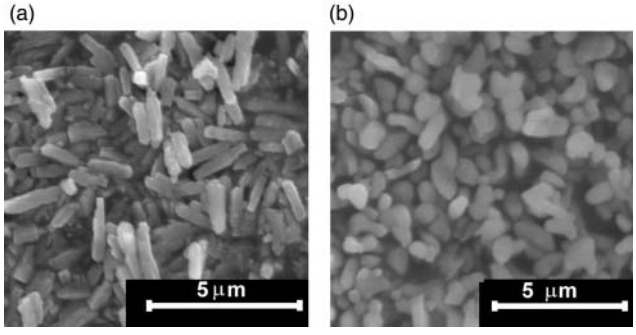

Fig. 5 SEM pictures of (a) cubic and (b) trigonal $ZrMo_2O_8$ prepared *via* the perchlorate route.

5. Conclusions

The preparation of phase pure cubic $ZrMo_2O_8$ is challenging as the material is metastable at all temperatures. Of the possible synthetic routes that were investigated, formation of cubic $ZrMo_2O_8$ was only observed on dehydration of $ZrMo_2O_7(OH)_2{\cdot}2H_2O$ *via* LT $ZrMo_2O_8$. The ease of obtaining pure cubic $ZrMo_2O_8$ depended intimately on the conditions used to prepare the hydrate. Good crystallinity hydrates facilitated the formation of cubic $ZrMo_2O_8$. Zirconyl perchlorate was found to be the most suitable precursor, followed by zirconyl nitrate and zirconyl chloride. A 1 : 2 metal ratio in the starting mixture led to lower crystallization temperatures for the cubic phase and helped avoid the cocrystallization of cubic and trigonal $ZrMo_2O_8$. However, all of these precipitates had a Zr : Mo ratio smaller than 1 : 2.

Stoichiometric $ZrMo_2O_7(OH)_2{\cdot}2H_2O$ prepared *via* the nitrate route (preparation with a large excess of Zr) always resulted in the cocrystallization of cubic and trigonal $ZrMo_2O_8$, while some of the chloride precursor samples and all of the samples prepared using the perchlorate route yielded pure cubic materials. Furthermore, the cubic samples prepared using the perchlorate route contained no amorphous material. The rod like particle shape, however, may lead to problems with respect to incorporation into controlled thermal expansion composites as well as high-pressure behavior under non-hydrostatic conditions.

Acknowledgements

This research was supported by the National Science Foundation through grant DMR-9623890 and the Office of Naval Research through the Molecular Design Institute at the Georgia Institute of Technology, which is supported under ONR contract N00014-95-1-1116. Acknowledgment is made to the donors of The Petroleum Research Fund, administered by the American Chemical Society, for partial support of this research under contract number 35087-AC5. The variable temperature XRD data were collected at Oak Ridge National Laboratory, sponsored by the Assistant Secretary for Energy Efficiency and Renewable Energy, Office of Transportation Technologies, as part of the High Temperature Materials Laboratory User Program, Oak Ridge National Laboratory, managed by UT-Battelle, LLC, for the US Dept. of Energy under contract DE-AC05-00OR22725. We are grateful to the Georgia Tech Microscopy Center for providing the research facilities used in the microstructural characterization and to the Textiles and Fiber Engineering Thermal Analysis Center for access to the thermal analysis equipment.

References

1 A. W. Sleight, *Inorg. Chem.*, 1998, **37**, 2854.
2 A. W. Sleight, *Ann. Rev. Mater. Sci.*, 1998, **28**, 29.
3 J. S. O. Evans, *J. Chem. Soc., Dalton Trans.*, 1999, 3317.
4 D. A. Fleming, D. W. Johnson and P. J. Lemaire, *Article Comprising a Temperature Compensated Optical Fiber Refractive Index Grating*, *US Pat.,* 5,694,503, 1997.
5 C. E. Guillaume, *C. R. Acad. Sci.*, 1897, **125**, 235.
6 F. A. Hummel, *J. Am. Ceram. Soc.*, 1951, **34**, 235.
7 J. P. Boilot and J. P. Salanie, *Mater. Res. Bull.*, 1979, **14**, 1469.
8 S. Y. Limaye, D. K. Agrawal, R. Roy and Y. Mehrotra, *J. Mater. Sci.*, 1991, **26**, 93.
9 R. Roy, D. K. Agrawal and H. A. McKinstry, *Annu. Rev. Mater. Sci.*, 1989, **19**, 59.
10 G. K. White, *Contemp. Phys.*, 1993, **34**, 193.
11 C. Verdon and D. C. Dunand, *Scr. Mater.*, 1997, **36**, 1075.
12 H. Holzer and D. C. Dunand, *J. Mater. Res.*, 1999, **14**, 780.
13 J. S. O. Evans, T. A. Mary and A. W. Sleight, *J. Solid State Chem.*, 1997, **133**, 580.
14 J. S. O. Evans, T. A. Mary and A. W. Sleight, *J. Solid State Chem.*, 1998, 137.
15 P. M. Forster, A. Yokochi and A. W. Sleight, *J. Solid State Chem.*, 1998, **140**, 157.
16 T. A. Mary and A. W. Sleight, *J. Mater. Res.*, 1999, **14**, 912.
17 V. Korthuis, N. Khosrovani, A. W. Sleight, N. Roberts, R. Dupree and W. W. Warren, *Chem. Mater.*, 1995, **7**, 412.
18 N. Khosrovani, V. Korthuis, A. W. Sleight and T. Vogt, *Inorg. Chem.*, 1996, **35**, 485.
19 J. S. O. Evans, J. C. Hanson and A. W. Sleight, *Acta Crystallogr., Sect. B*, 1998, **54**, 705.
20 J. S. O. Evans, T. A. Mary, T. Vogt, M. A. Subramanian and A. W. Sleight, *Chem. Mater.*, 1996, **8**, 2809.
21 T. A. Mary, J. S. O. Evans, T. Vogt and A. W. Sleight, *Science*, 1996, **272**, 90.
22 C. Closmann and A. W. Sleight, *J. Solid State Chem.*, 1998, **139**, 424.
23 C. Lind, A. P. Wilkinson, Z. Hu, S. Short and J. D. Jorgensen, *Chem. Mater.*, 1998, **10**, 2335.
24 C. Martinek and F. A. Hummel, *J. Am. Ceram. Soc.*, 1968, **51**, 227.
25 J. S. O. Evans, Z. Hu, J. D. Jorgensen, D. N. Argyriou, S. Short and A. W. Sleight, *Science*, 1997, **275**, 61.
26 Z. Hu, J. D. Jorgensen, S. Teslic, S. Short, D. N. Argyriou, J. S. O. Evans and A. W. Sleight, *Physica B*, 1998, **241–243**, 370.
27 C. Lind, D. G. VanDerveer, A. P. Wilkinson, J. Chen, M. T. Vaughan and D. J. Weidner, *Chem. Mater.*, 2001, **13**, 487.
28 A. Clearfield and R. H. Blessing, *J. Inorg. Nucl. Chem.*, 1972, **34**, 2643.
29 A. C. Larson and R. B. Von Dreele, *GSAS—General Structure Analysis System*, Report LA-UR-86-748, 1987.
30 E. A. Payzant and W. S. Harrison, *Adv. X-Ray Anal.*, 2000, **43**, 267.
31 H. Wang and E. A. Payzant, *Proc. SPIE*, 1999, 377.